Available online at www.sciencedirect.com
SCIENCE DIRECT®
International Journal of Thermal Sciences 44 (2005) 953–965
International Journal of Thermal Sciences
www.elsevier.com/locate/ijts

Flash evaporation from a water pool: Influence of the liquid height and of the depressurization rate

D. Saury *, S. Harmand, M. Siroux

Laboratoire de Mécanique et Énergétique, Université de Valenciennes et du Hainaut Cambrésis, Le Mont Houy, 59313 Valenciennes cedex 9, France

Received 18 March 2004; received in revised form 24 February 2005; accepted 7 March 2005

Available online 10 May 2005

Abstract

This article presents a study about the influence of the initial water height and of the depressurization rate on the flash evaporation of a water film. Experimental study is carried out with initial water height ranging from 25 to 250 mm, superheats between 2 and 44 K, and an initial liquid temperature from 45 to 85 °C. Visualization of the phenomenon using a CCD camera lets us firstly point out the influence of the initial water level on the flashing phenomenon in a qualitative way. Thermal balance allows us to correlate the mass evaporated with the liquid temperature, and then to quantify the influence of the initial water height on several parameters: maximal amplitude of the phenomenon, flashing time, liquid mass evaporated. We also analyse influence of relatively low depressurization rate (from 0 to 3.5 bar·s^{-1}) on the flashing time, the mass evaporated, and the mass flow rate. Finally, dimensionless correlations between these parameters are proposed.

Keywords: Flash evaporation; Liquid height; Depressurization rate; Flashing time; Superheat; Evaporated mass

1. Introduction

Evaporation flash, or flashing, is the phenomenon observed when the surrounding liquid conditions suddenly change and become lower than its saturated conditions. Due to the sudden variation of the conditions, the liquid initially at equilibrium becomes superheated. This is, for instance, the case of suddenly depressurized liquids below the saturation pressure corresponding to their initial temperature. Due to the sudden drop in pressure, the whole energy cannot be contained in the liquid as sensible heat, and the heat surplus is converted into latent heat of vaporization. A violent phase change is then observed. This is at the origin of the vapor bubbles formation inside the liquid bulk and its vaporization. Moreover, due to the sudden vaporization, the temperature of the liquid decreases quickly.

Industrial applications of flashing are varied. One of the most important concerns the sea water desalination for drinking water production. In this case, multistage flash evaporators are generally used [1], but hybrid systems combining flashing and energy storage appear [2].

Drying processes also use this phenomenon. For instance, sterile loads drying in vapor sterilization cycles [3], or paper sheet drying [4] use flashing.

Due to the sudden phase change, flash evaporation phenomenon causes a sudden temperature drop of the liquid. This ability to quickly cool is highly used in industrial processes such as the cooling of hot parts of a shuttle by water spraying under low pressure conditions [5,6], or the grape cooling in wine manufacturing process [7].

Flash evaporation phenomenon is also used in geothermal power plants to generate vapor which drives the turbines producing electricity. The OTEC like—ocean thermal energy conversion—power plants use the fact that water layers in oceans are at different temperatures to produce energy [8,9].

The phenomenon can also occur in nuclear power plants with the break of the core reactor cooling system. This is known as loss of coolant accident or LOCA. In this case, the high pressure cooling agent is directly in contact with the surrounding environment at atmospheric pressure. It then explodes into vapor due to the flash evaporation [10].

* Corresponding author. Fax: +33 3 27 51 19 61.
E-mail address: didier.saury@univ-valenciennes.fr (D. Saury).

1290-0729/$ – see front matter
doi:10.1016/j.ijthermalsci.2005.03.005

Nomenclature

A	horizontal cross-sectional area of the flash chamber	m^2	
C	salt concentration	%	
c_p	specific heat of liquid at constant pressure	$J{\cdot}kg^{-1}{\cdot}K^{-1}$	
c_v	specific heat of liquid at constant volume	$J{\cdot}kg^{-1}{\cdot}K^{-1}$	
H	initial water height	m	
H_{crit}	critical water height	m	
h_{fg}	latent heat of vaporization	$J{\cdot}kg^{-1}$	
m	water mass	kg	
p	pressure	Pa	
q	mass flow rate	$g{\cdot}s^{-1}$	
T	temperature of water	°C	
t	time	s	
t^*	flashing time	s	
V	volume of the water	m^3	
v_p	depressurization rate	$bar{\cdot}s^{-1}$	
Greek symbols			
Δp	pressure drop	Pa	
ΔT	superheat	K	
λ	liquid thermal conductivity	$W{\cdot}m^{-1}{\cdot}K^{-1}$	
ρ	density	$kg{\cdot}m^{-3}$	
σ	liquid surface tension	$N{\cdot}m^{-1}$	
Subscripts and superscripts			
0	initial state		
$*$	state at t^*		
e	equilibrium		
ev	evaporated		
f	final state		
l	liquid phase		
max	maximum value		
sat	condition of saturation		
Dimensionless numbers			
Ja	Jakob number		
NEF	non-equilibrium function		
Pr	Prandtl number		
$\overline{X}$	dimensionless quantity related to the X quantity		

Flash evaporation is also used in some multi-components film deposition processes [11] where a liquid multi-components mixture is evaporated and then condensate again as thin layer on the substrate surface.

In a general way, flashing is a process which allows vaporization rates more significant than those obtained with the conventional evaporation [12]. Phenomenon is often used as soon as a large amount of vapor must be produced, or when fast cooling is necessary. Also, aiming at a better knowledge of this phenomenon, this work study the evolution of some parameters such as the flashing time, or the water mass evaporated. Influence of both the initial liquid level and the depressurization rate on the flash evaporation phenomenon from water pool are poorly documented in literature. Also in this article, we propose an analysis of these two parameters.

2. Literature survey

2.1. Mass evaporated by flashing

In order to have a better understanding of the flash evaporation phenomenon, Miyatake et al. [13,14] carried out experiments on a pure water pool in which initial water heights range from 100 to 225 mm, equilibrium temperature varies between 40 and 80 °C, and superheat from 2.5 to 5.5 K. Using a global energy balance that supposes the whole energy released by the liquid cooling is used to vaporize it, and considering as constant the fluid properties (ρ_l, c_p and h_{fg}) and the volume of liquid since the evaporated mass is not very significant when compared to the initial water mass, they obtained a relationship between the mass evaporated and the liquid temperature:

$$m_{ev}(t) = \frac{\rho_l V_0 c_p}{h_{fg}}\big[T_0 - T(t)\big] \tag{1}$$

Gopalakrishna et al. [15,16] work on sea water desalination. Aiming at that, they carried out experiments with an initial temperature from 25 to 80 °C, superheats between 0.5 and 10 K, an initial liquid heights of 165, 305 and 457 mm, the salt concentration of the water varying from 0 to 3.5%. By measuring the liquid level with a cathetometer, they propose the following correlation connecting the mass evaporated to various parameters described below:

$$m_{ev}(t) = m_v C_1 Ja_p^{0.05} Pr^{-0.05}\left(\frac{\Delta p'}{H}\right)^{-0.03} \times (1+C)^{0.06}\big[1-\exp(-p_2 t)\big] \tag{2}$$

where $\Delta p'$ corresponds to the drop in pressure. It is thus expressed in water millimeter (mm_{H_2O}), i.e., $\Delta p' = \frac{\Delta p}{\rho g}$. C is the salt concentration in percent [%]. Other physical quantities or terms are proposed below and must be expressed in SI units

$$p_2 = \frac{0.27}{\tau} Ja_p^{0.133}\left(\frac{\Delta p'}{H}\right)^{-1.6}$$

$$Ja_p = c_p T_0 \Delta p \frac{\rho_l/\rho_v^2 - 1/\rho_v}{h_{fg}^2}$$

$$m_v = Ja\, A H \rho_l$$

$$Ja = \frac{c_p \Delta T}{h_{fg}}, \qquad \tau = \frac{(\sigma/\Delta p)^2}{\lambda/\rho c_p}, \qquad C_1 = 0.8867$$

The range of validity for this correlation is given below:

$$0.1116 \leqslant \frac{\Delta p'}{H} \leqslant 2.615, \qquad 0 \leqslant C \leqslant 0.035$$
$$12 \leqslant Ja_p \leqslant 197, \qquad 2.706 \leqslant Pr \leqslant 5.941$$

More recently, in a previous article (Saury et al. [17]), we presented results about the flash evaporation of a water film of 15 mm. The evaporated mass is obtained using the heat balance on the liquid in the flash chamber. This mass is then compared with correlation proposed by Gopalakrishna et al. [15,16] when possible. We also highlighted the influence of superheat on the final evaporated mass and on the flashing time. Lastly, we strongly enlarged the domain of study since, in our experiments, superheat ranges between 1 and 35 K.

2.2. NEF: Non-equilibrium function and flashing time

In its investigation about flash evaporation, Miyatake [13] defined NEF (non-equilibrium function) as:

$$NEF(t) = \frac{m_{\mathrm{ev}}(\infty) - m_{\mathrm{ev}}(t)}{m_{\mathrm{ev}}(\infty)} \tag{3}$$

where $m_{\mathrm{ev}}(\infty)$ corresponds to the ideal mass evaporated when the liquid goes from the initial temperature T_0 to the equilibrium temperature $T_e = T_{\mathrm{sat}}(p_e)$. Thus, considering than the volume of liquid changes very slightly and using Eq. (1), we can also write:

$$NEF(t) = \frac{T(t) - T_e}{T_0 - T_e}, \quad \text{where } T_e = T_{\mathrm{sat}}(p_e) \tag{4}$$

The typical evolution of the NEF with time shows two exponential decays. The curve plotting the NEF versus time can then be divided in two parts: a first part of strong slope followed by a more gradual one. Intersection of these two slopes gives what we call the flashing time, often noted t^*. The first phase corresponds to a vigourous boiling in the whole liquid bulk.

2.3. Importance of the depressurization rate on the phenomenon

Hahne and Barthau [18] note that when a liquid in equilibrium with its vapor and placed in a closed tank is suddenly depressurized, this latter enters in a metastable state (superheated) which mainly depends on the pressure drop and flashing phenomenon appears. Parameters influencing such a phenomenon are the pressure drop, the rate of depressurization and the initial temperature [18,19]. Experiments carried out by Hahne and Barthau concern relatively low depressurization rates (some bar·s^{-1}) in hyperbaric surrounding for various liquids (water, Refrigerant 11). They remark that flashing occurs for such depressurization rates and even if this depressurization is applied to a liquid put in a significant diameter enclosure (at least up to 250 mm). Moreover, they notice that when the rate of depressurization increases, the phenomenon happens more quickly. This is well shown

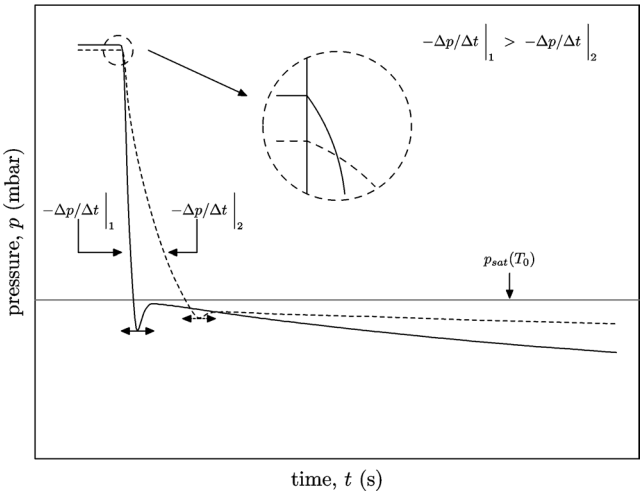

Fig. 1. Typical evolution of the pressure during the initial phase of depressurization with two different depressurization rates.

on Fig. 1 which plots the evolution of the pressure versus time that can be typically observed for two different rates of depressurization and which is drawn using our data. The initial evolution with time observed by many authors [18,19] is well point up. The value of the local minimum of pressure (reached initially) is lower and sooner when the rate of depressurization increases. The presence of this local minimum could be explained by the rate of generation of vapor (vapor outflow) due to fast nucleation in the whole liquid, which compensates and even exceeds during a short time the rate of depressurization.

Principal studies found in literature [20–24] generally relate to depressurizations of flowing liquids (water, R-134a, butane, propane, ...) initially pressurized (some bars) until an equilibrium pressure which is often 1 bar (release to the atmosphere of a pressurized liquid). Under such conditions, the depressurization rates are high (from 100 atm·s^{-1} to some Matm·s^{-1}). However all authors are unanimous for saying the appearance of the flashing strongly depends on the depressurization rate. Until now, few studies concerning the brutal depressurization to low pressures (about a few tens of millibars) for a liquid placed in a tank were carried out.

In literature, many different initial water heights are used to study flash evaporation phenomenon from pool, but few of them deal with the influence of this height on the properties of the flash evaporation such as the flashing time or the mass evaporated. All in all, studies available in literature concern water heights varying from 15 to 457 mm, initial temperatures from 25 to 80 °C, and superheats from 0.5 to 35 K. Table 1 gathers these values, those concerning our previous article on this subject [17] and those studied in this present investigation of the initial water level influence. Moreover, we also noticed that few authors studied influence of the depressurization rate on flashing phenomenon, especially for low ranges of depressurization rate. In order to fill this gap, we also propose an experimental study the influence of the

Table 1
Key parameters used by main authors

	Miyatake (1973–1977)	Gopalakrishna (1987)	Saury (2002)	This study
T_e [°C]	40–80	–	–	–
T_0 [°C]	–	25–80	30–75	45–85
ΔT [K]	2.5–5.5	0.5–10	1–35	2–44
H [mm]	100–225	165, 305, 457	15	25–250
p_0 [mbar]	73–473[a]	30–310[a]	50, 100, 150, 200	50, 150

[a] These estimated values are based on data provided by the authors.

low rates of depressurization (some bar·s^{-1}) on the kinetic of the flash evaporated quantities.

3. Experimental setup

3.1. Test procedure

The experimental setup is shown on Fig. 2. Fig. 3 presents thermocouples and pressure transducer placement in the flash chamber and specifies the flash chamber dimensions.

First step of the test procedure consists in fill in the flash chamber with distilled water up to the right initial level. This water is then warmed up by the heating power and degased by successive drops in pressure in order to avoid the greater number of parasitic nucleation sites. Once water is at the correct temperature, the electromagnetic valve is closed. Then liquid ring pump lets obtain desired pressure into the vacuum tank. Once these pressure is reached, the flow control valve is adjusted if necessary and images and measurements acquisition chains are started. Flash chamber and vacuum tank are then suddenly put into communication by opening the electromagnetic valve: flashing start.

3.2. Set-up instrumentation

Liquid and vapor temperatures are measured by six 0.08 mm diameter type T thermocouples (cf. Fig. 3). Type T was selected because of its good reaction to vacuum and humidity. It can measure temperatures from −270 to +400 °C, its precision is of 0.12 °C and its response time of 40 ms.

Pressure in the flash chamber and vacuum tank is measured by two pressure transducers. The first one is a piezoresistive sensor in stainless steel which measures absolute pressure on a 1.5 bar range. Its temperature range is from 20 to 100 °C. Its bandwidth is 13 kHz and its precision 1% of its measurement range. The second one is an active strain gauge. Its effective measurement range is from atmospheric pressure (1000 mbar) to 10^{-1} mbar. Its precision is ±0.2% of its measurement range.

The data acquisition system (HP75000B) is controlled by a PC via a HP-IB bus. Thermocouples are connected to this data logger using a HP-E1347A card and the connection between the pressure transducers and recorder is carried out by a HP-E1345A card.

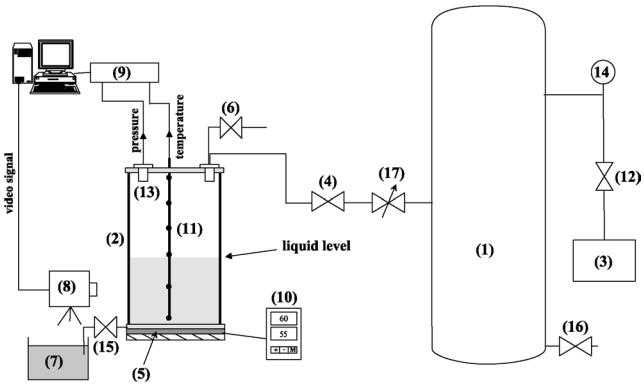

Fig. 2. Experimental setup description. (1) Vacuum tank; (2) Flash chamber; (3) Vacuum pump; (4) Electromagnetic valve; (5) Heating power; (6) Aerating valve; (7) Distilled water tank; (8) Digital CCD camera; (9) Data acquisition unit; (10) Temperature regulator; (11) Thermocouples; (12) Insulation valve; (13) Pressure transducer; (14) Pressure transducer; (15) Drain out valve; (16) Drain out valve; (17) Flow control valve.

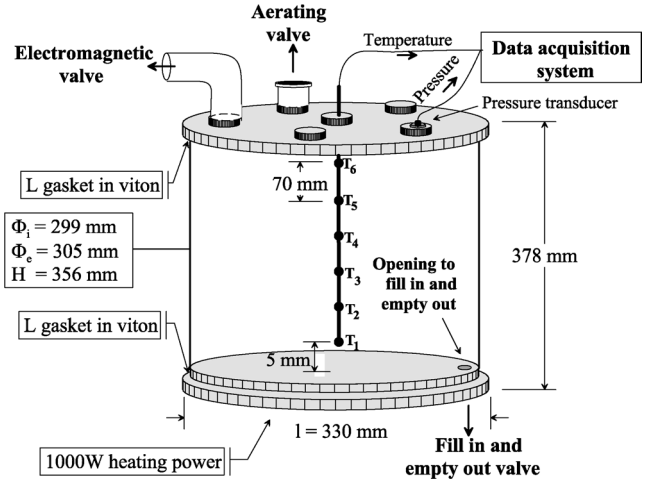

Fig. 3. Flash chamber description.

A digital CCD camera CVM70 which lets obtain up to 6 frames per second is used. This camera is connected to a computer and controlled using the software Optimas©.

3.3. Evaporated quantities determination

Method used to calculate the water mass evaporated by flashing is based on an energy balance on the liquid in flash chamber. Between two close times, this liquid is supposed to be in equilibrium with its produced vapor and incompressible. Studied system can be divide into two sub-systems in equilibrium. The first one is composed with a mass $m - \mathrm{d}m$ of liquid at the temperature T at time t which is converted, at time $t + \mathrm{d}t$, into a mass $m - \mathrm{d}m$ of liquid at the temperature $T + \mathrm{d}T$. The second sub-system, is composed by a mass $\mathrm{d}m$ of liquid at the temperature T at time t and by a mass $\mathrm{d}m$ of vapor at the temperature $T + \mathrm{d}T$ at time $t + \mathrm{d}t$. Neglecting thermal loss with walls and with the surrounding fluid and neglecting the second order terms, we obtained the following heat balance:

$$mc_v\,\mathrm{d}T - \mathrm{d}m\,h_{\mathrm{fg}} = 0 \tag{5}$$

Integrating over the time, we obtain the evolution of the mass evaporated with time. Due to the low temperature range, the properties of the liquid—ρ_l, h_{fg}, c_v—are supposed constant during phenomenon. So, the following equation is then obtained:

$$m_{\mathrm{ev}}(t) = \rho_l A H \left\{ 1 - \exp\left[-\frac{c_v}{h_{\mathrm{fg}}}(T_0 - T) \right] \right\} \tag{6}$$

Deriving this equation over the time, and considering fluids physical properties as constants, the evaporated mass flow rate is also obtained.

$$\dot{m}_{\mathrm{ev}}(t) = \frac{\mathrm{d}m_{\mathrm{ev}}}{\mathrm{d}t}(t) = -\rho_l A H \left(\frac{c_v}{h_{\mathrm{fg}}} \right) \exp\left[-\frac{c_v}{h_{\mathrm{fg}}}(T_0 - T) \right] \frac{\mathrm{d}T}{\mathrm{d}t} \tag{7}$$

Uncertainty on the mass evaporated obtained using Eq. (6) is studied in [25], and shows that this relative uncertainty remains lowers than 12%.

4. Results and analysis

4.1. Description of the phenomenon

Images acquire using CCD Camera shows that the phenomenon is initially very violent: the liquid is completely disrupted and bubbles formation takes place in the whole liquid volume. After a relatively short period of intense boiling, phenomenon magnitude decreases, and boiling only occurs closer and closer to the free surface. Then liquid temperature in the flash chamber tends towards equilibrium which corresponds to the saturation temperature of the liquid at the equilibrium pressure of the flash chamber. Evolution of the phenomenon with time can be explained by the pressure distribution in the flash chamber and especially in the liquid. Indeed, pressure in the liquid phase increases with depth, thus the farther from surface, the more the effective pressure drop $\Delta p = p_{\mathrm{sat}}(T_0) - p_e \approx p_{\mathrm{sat}}(T_0) - p_{\mathrm{sat}}(T_e)$ at the origin of the flash evaporation phenomenon decreases and the more the local equilibrium temperature of the liquid—which corresponds to the liquid saturation temperature—increases. This equilibrium temperature will thus be reached firstly in places where the pressure is the most significant, i.e., at the bottom of the flash chamber. So, during flashing, due to the abrupt pressure drop, liquid cools quickly and the deepest water layers reach an equilibrium state faster. Flashing stops then gradually from the flash chamber bottom upwards the surface where the phenomenon continues and where the upper water layers keep on cooling. The hottest—and thus less dense—water layers are at the bottom of the tank. They naturally move upwards and supply an additional energy contribution as sensible heat. This explains why the closer we are to the surface of the liquid, the more the phenomenon will be sustained. In addition, since local equilibrium temperature increases with depth, local liquid superheat decreases and in some cases (low superheats and/or great water heights), the deep water layers can already be at equilibrium. On the other hand, the closer to the surface, the more significant the superheat, which explains the violence of the flash evaporation phenomenon observed up to there. Moreover, movements created by the displacement of the layers at different temperatures contribute to homogenize the liquid temperature. This homogenisation is of course reinforced by the formation and the growth of vapor bubbles which are formed due to flashing and which mix the whole liquid. Combination of these phenomena explains what we observe experimentally, namely an initial phase of very intensive boiling which disrupts the whole volume of superheated liquid followed by a phase whose magnitude decreases with time and depth.

4.2. Influence of the initial water level on flashing phenomenon

4.2.1. Qualitative analysis

In order to study the influence of initial liquid height on the flashing time, we observe the state of the liquid initially at 60 °C and suddenly depressurizes down to 150 mbar 15 seconds after the beginning of the phenomenon for initial heights ranging between 50 and 250 mm. Time $t = 15$ s is chosen because, as it will be see later, it corresponds to the average flashing time obtained for this series of experiments. As we can note it, the higher the initial water level in the flash chamber, the more violent and of great amplitude the phenomenon is at this moment. However as we explained before, amplitude of the phenomenon decreases with time. We can thus deduce that the higher the water level, the less achieved the phenomenon is at time $t = 15$ s or, to put it in another way, phenomenon duration increases with height. Thus flashing time seems to be an increasing function of the initial liquid level. This can be explained by the fact that increasing the initial water level in the flash chamber involves a growth in initial water mass and thus increases the energy supplied as sensible heat. This latter must be converted into latent heat, and consequently water inertia involves an increase of the flashing time.

In order to confirm observations made previously using the images analysis, experiments with an initial pressure in the vacuum tank of 50 and 150 mbar, an initial temperature from 45 to 85 °C, and an initial height of water ranging between 25 and 250 mm were carried out. These experiments correspond to superheats from 2 to 44 K. All the curves presented hereafter and using temperature measurements are plotted using data of the thermocouple called T_1 in Fig. 3 since this thermocouple is, whatever the run, the only one which is always underwater. Moreover, choice of this thermocouple is justified by the violence of the phenomenon which, during the flashing, involves a significant mixing of the liquid and thus a quasi-homogeneous distilled water temperature in the flash chamber. Fig. 4 presents the evolution of the liquid temperature when flashing occurs for underwa-

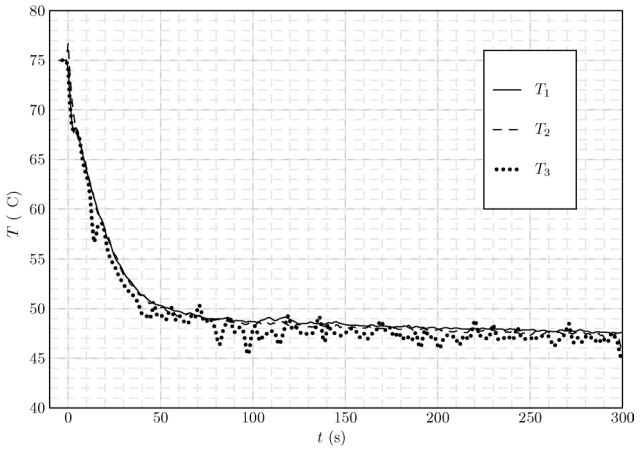

Fig. 4. Temperature measurement into the flash chamber using underwater thermocouples T_1 to T_3.

ter thermocouples called T_1 to T_3 in Fig. 3 with $T_0 = 75\,^{\circ}\mathrm{C}$, $p_0 = 50$ mbar, and $H = 150$ mm. Fluctuation observed on temperature profile measured using T_3 can be explained by the position of this thermocouple which is initially 5 mm under the free surface where phenomenon is longer and the more violent. Moreover, this graph shows that no thermal stratification is observed which can be explain by the violence of the phenomenon which disrupted the whole liquid bulk and by the bubble formation and growth which mixed the liquid. This point also confirm observation made by Kim et al. [26].

4.2.2. Influence of the initial water level on the violence of the phenomenon

Processing of the sequences of images lets determine the maximum amplitude $\Delta H_{\max}$ of flashing phenomenon for each run carried out. This magnitude corresponds to the difference between the maximum height reached by water in the tank while phenomenon occurs and the maximum depth reached by the bubbles in the liquid phase. Fig. 5 presents an annotated picture in order to have a better understanding on how $\Delta H_{\max}$ is determined. This amplitude allows to characterize the violence of the phenomenon since it is directly related to the liquid volume disrupted.

Fig. 6 presents the typical evolution of this amplitude with the initial height of liquid for an initial temperature of 75 °C and an initial pressure of 50 mbar. As we can note it, the maximum magnitude $\Delta H_{\max}$ of the phenomenon is an increasing function of the initial height. However, the low precision in the determination method of this amplitude coupled with a relatively low acquisition frequency of the CCD camera (7 Hz) does not allow us to continue our investigations in this way.

4.2.3. Influence of the initial water level on the flashing time

Fig. 7 shows the evolution of the flashing time t^* determined using *NEF*'s plot for initial pressures in the vacuum tank of 50 mbar and initial liquid temperature of 75 °C. The

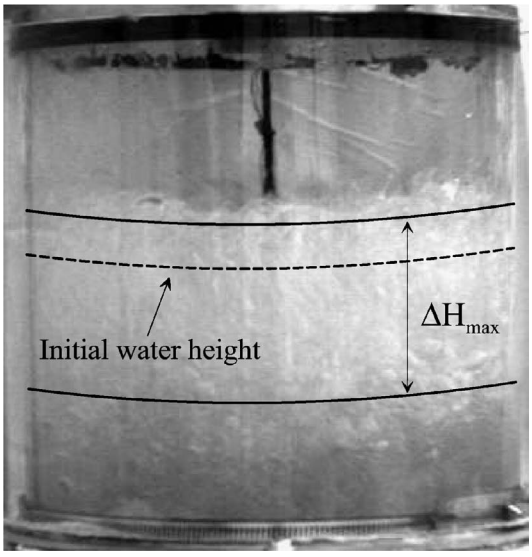

Fig. 5. Determination of maximum amplitude $\Delta H_{\max}$ of the flashing phenomenon.

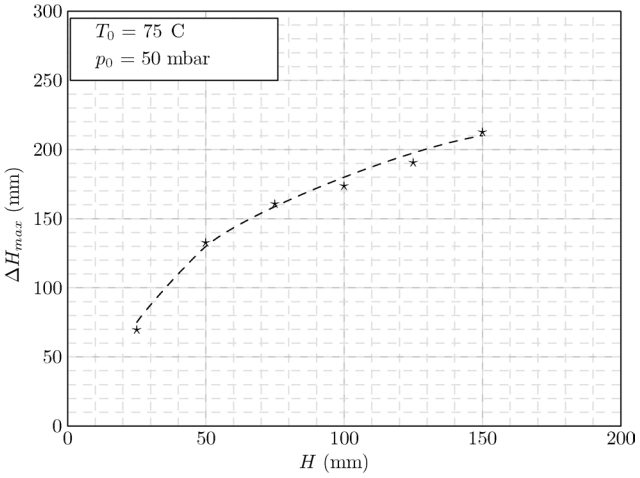

Fig. 6. Evolution of the maximum phenomenon amplitude for an initial pressure in the vacuum tank of 50 and an initial liquid temperature of 75 °C.

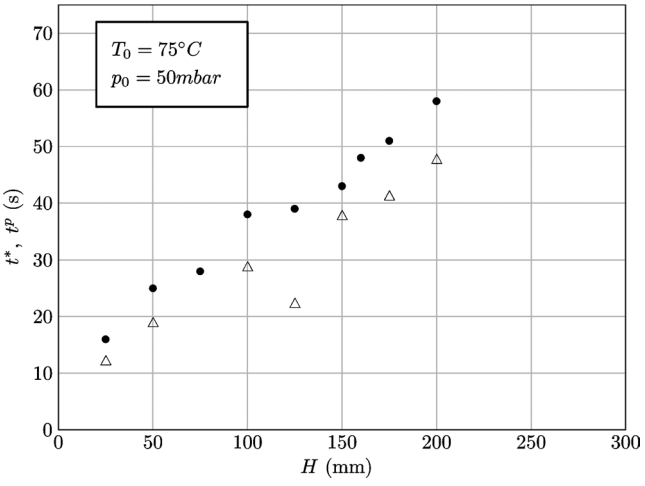

Fig. 7. Evolution of the flashing time t^* (•), and t^p (△) versus the initial height H for an initial temperature $T_0 = 75\,^{\circ}\mathrm{C}$ and $p_0 = 50$ mbar.

same trend is observed for a pressure of 150 mbar and for other temperatures. All in all, flashing time is an increasing function of the initial water level, which confirms the trend describes previously. This trend can be explained by the water inertia which increases with the initial height, since the water mass initially present and thus the energy to convert increases. It is to notice that the flashing time t^* increases when the initial pressure of the vacuum tank p_0 decreases. This is due to the fact that when p_0 decreases, the liquid superheat ΔT increases. Thus the amount of energy available as sensible heat for conversion into latent heat of vaporization is then greater. This involves a longer phenomenon.

In order to understand the magnitude order found, another characteristic time, noted t^p is calculated. To find this time, we study the dimensionless and normalized pressure evolution p_{adim} versus time. This quantity is defined as follow:

$$p_{\text{adim}}(t) = \frac{p(t) - p_e}{p_{\text{sat}}(T_0) - p_e} \tag{8}$$

Lets ξ the initial slope of the curve plotting p_{adim} versus time, t^p is defined as $t^p = -1/\xi$. On Fig. 7, we also overwrite values obtained for t^p and for t^*. As observed, whatever initial conditions, values obtained are on the same order of magnitude. Moreover, we could also observe these values are very close for small superheats, and a slightly more scattered for greater superheats values. This point could be explained by the violence of the phenomenon which could disturb pressure measurement. So, characteristic time found using temporal pressure evolution t^p, highlight the influence of the vapor space pressure variation on the characteristic time of the phenomenon and confirms what Gopalakrishna observed [16], i.e., the rate of pressure reduction in the vapor space could be a significant factor controlling the process. Influence of this depressurization rate will be discussed later.

4.2.4. Influence of the initial level on the water mass evaporated by flashing

Heat balance applied to the liquid enables us to connect the mass evaporated by flashing m_{ev} to the temperature of the liquid (see Eq. (6)). This mass is calculated using Eq. (6) and the evolution of the liquid temperature with time given by the thermocouple called T_1. Typical evolution of this quantity shows this mass increases very quickly at the beginning ($t < t^*$) while its evolution stops for times greater than the flashing time and tends towards a limiting value. Thus total mass evaporated by flashing during an experiment m^f_{ev} corresponds to the limit value of this curve.

Figs. 8 shows results obtained for the final mass evaporated with initial pressures in the vacuum tank of respectively 50 mbar, initial temperatures from 45 to 85 °C, and initial water heights ranging between 25 and 250 mm. The same trend as for $p_0 = 50$ mbar is observed for other initial pressure ($p_0 = 150$ mbar). Whatever the run, final evaporated mass is an increasing function of the initial temperature and of the initial level of water in the flash chamber.

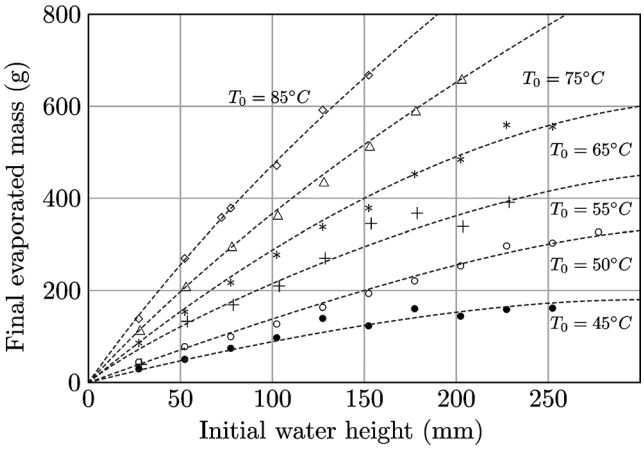

Fig. 8. Evolution of the final mass evaporated versus time for $p_0 = 50$ mbar.

General trends of these curves were approached and plotted on these figures. We can notice using these curves that $\mathrm{d}m^f_{\text{ev}}/\mathrm{d}H > 0$ and $\mathrm{d}^2m^f_{\text{ev}}/\mathrm{d}H^2 < 0$ (increasing and concave profiles). This behavior can be explain by the effective pressure drop. Indeed, during a run, pressure drop entailing phenomenon goes from the saturation pressure at the initial temperature $p_{\text{sat}}(T_0)$ to the equilibrium pressure p_e which corresponds to the saturation pressure at the equilibrium temperature: $p_e = p_{\text{sat}}(T_e)$. For depths greater than $H_{\text{crit}} = \frac{p_{\text{sat}}(T_0) - p_{\text{sat}}(T_e)}{\rho g}$, liquid is already at equilibrium since its pressure is greater than $p_{\text{sat}}(T_e)$ and flashing does not occurs. This critical height increases very quickly with the initial temperature and the initial pressure. For instance, this critical height for the run with $T_0 = 45\,^\circ\text{C}$ and $p_0 = 50$ mbar ($\Delta T = 5$ K) is 233 mm. It corresponds on Fig. 8 to the height where the final mass evaporated no more increases. For the run with $T_0 = 50\,^\circ\text{C}$ and $p_0 = 50$ mbar ($\Delta T = 9$ K), $H_{\text{crit}} = 464$ mm, and for $T_0 = 60\,^\circ\text{C}$ and $p_0 = 150$ mbar ($\Delta T = 4$ K), $H_{\text{crit}} = 356$ mm. Considering the water heights to take into account and the current setup geometry, we can unfortunately not confirms experimentally the trends observed.

Fig. 9 represents the evolution of the ratio between the mass evaporated at t^* and the initial mass m_0 versus the Jacob number *Ja*, a dimensionless number relative to superheat, for an initial pressure in the vacuum tank of 50 and 150 mbar. On this figure, we can note that m^*/m_0 is proportional to *Ja*, and that this proportionality factor strongly depends on the initial pressure of the vacuum tank p_0. Indeed, this coefficient is about 0.91 for $p_0 = 50$ mbar and 0.55 for $p_0 = 150$ mbar. Thus it seems that the more significant the pressure drop Δp, the greater the proportionality factor.

Fig. 10 plots the evolution of the ratio between the final mass evaporated m^f_{ev} and the initial mass m_0 versus superheat ΔT of the liquid for an initial pressure in the vacuum tank of 50 and 150 mbar. We also plot results obtained using Eq. (2) proposed by Gopalakrishna. On this figure, we notice that m^f_{ev}/m_0 is proportional to ΔT, since when t goes to

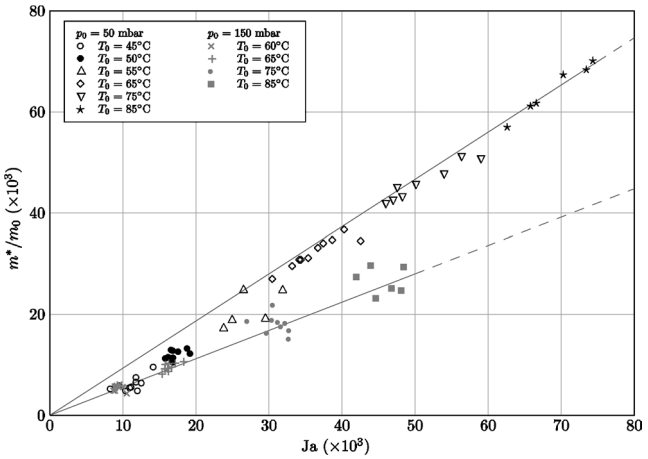

Fig. 9. Evolution of m^*/m_0 versus the Jakob number for $p_0 = 50$ mbar and $p_0 = 150$ mbar.

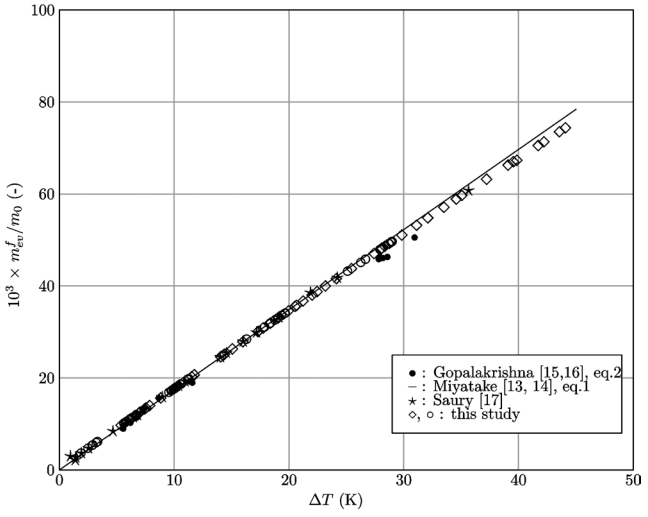

Fig. 10. Evolution of m^f_{ev}/m_0 versus ΔT for $p_0 = 50$ mbar (◇) and $p_0 = 150$ mbar (○).

infinity, T and m_{ev} respectively goes to T_e and m^f_{ev}, and, as $h_{fg} \gg c_v \Delta T$, Eq. (6) becomes (at first order):

$$\frac{m^f_{ev}}{m_0} = \frac{c_v}{h_{fg}} \Delta T \tag{9}$$

This explain the linear behavior observed on this graph. Moreover, values obtained are close to those proposed by Gopalakrishna, and slightly lower than those found using Miyatake's correlation (see Eq. (1)). Indeed, in our correlation, we take into account the mass variation during phenomenon occurs. So it is not surprising to obtain a lower mass evaporated than Miyatake. Moreover, unlike what we observed on Fig. 9, this ratio no more depends on the initial pressure which confirm the paramount influence of the superheat on this quantity.

Fig. 11 shows the evolution of the ratio between the mass evaporated at t^* and the total mass evaporated m^f_{ev} versus the superheat for initial pressures in the vacuum tank of 50 and 150 mbar. This ratio reflects well the effectiveness of

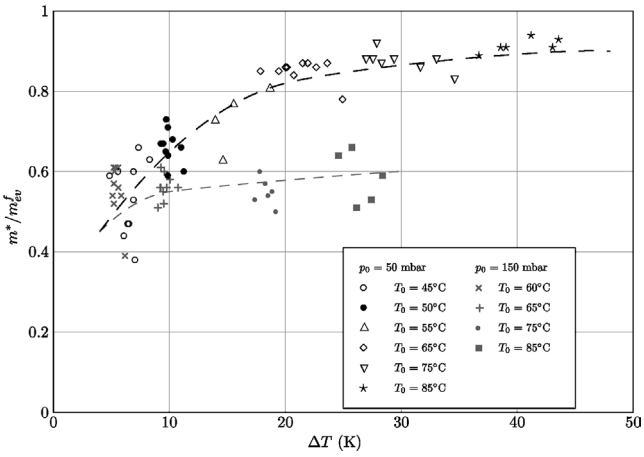

Fig. 11. Evolution of m^*/m^f_{ev} versus ΔT for $p_0 = 50$ mbar and $p_0 = 150$ mbar.

the phenomenon. Indeed, for an initial pressure in the vacuum tank of 50 mbar, the greater the superheat, the closer the mass evaporated at time t^* to the evaporated total mass, whatever the initial height of water in the flash chamber. For $p_0 = 150$ mbar, this ratio remains quasi-constant around 55% whatever the initial height of water, which shows thus the significative influence of the pressure drop Δp on evaporated quantities at time t^* and the influence of the initial water height. Moreover, for the same superheat this ratio increases with pressure drop whatever the initial height of water. Indeed, this ratio seems to be an increasing function of the pressure drop since this coefficient is close to 1 when the effective pressure drop Δp increases. Thus the increase of Δp seems to result in a more efficient phenomenon since m^* tends towards m^f_{ev}.

4.3. Influence of the depressurization rate on flashing phenomenon

4.3.1. NEF evolution with time

Fig. 12 presents the evolution of the NEF with time for an initial temperature of 75 °C, initial pressure p_0 of 50 mbar, and initial water heights of 25 and 250 mm. For other initial heights (25 to 250 mm), initial pressure (150 mbar) and initial temperatures (60, 75 and 85 °C), curves are not presented in this article, but the same trend is however observed.

Firstly, we observe that NEF is a decreasing function of time well pointing out the temperature drop of the liquid. Moreover, whatever the initial water height, we note that the cooling, caused by the evaporation of the liquid, is slower when the depressurization rate decreases. Indeed, the temperature drop (which is directly connected to the evolution of NEF) is slower when this rate of depressurization ($v_p = -\mathrm{d}p/\mathrm{d}t$) is lowered. In addition, for depressurization rates of the same order of magnitude, we can observe a liquid temperature profile more square when the water height decreases. In another words, it seems that for the same rate of depressurization, equilibrium is reached faster when the

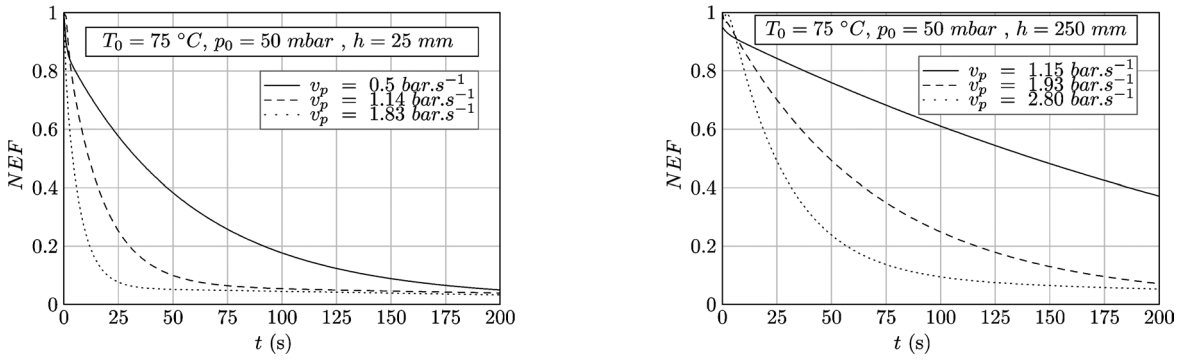

Fig. 12. NEF evolution with time for $T_0 = 75\,°C$, $p_0 = 50$ mbar, and $h = 25$ and 250 mm.

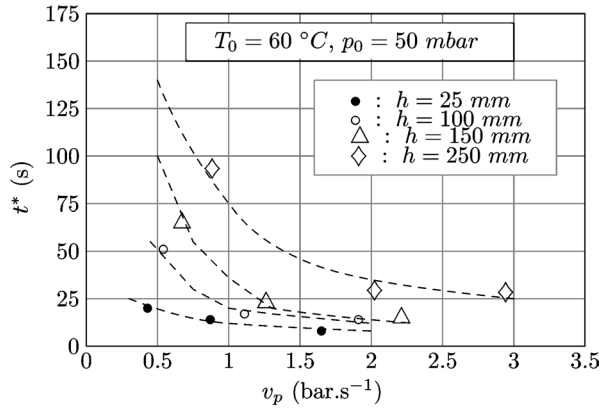

Fig. 13. Evolution of the flashing time with the rate of depressurization for an initial pressure in the vacuum tank of 50 mbar and different initial temperatures and initial levels of liquid.

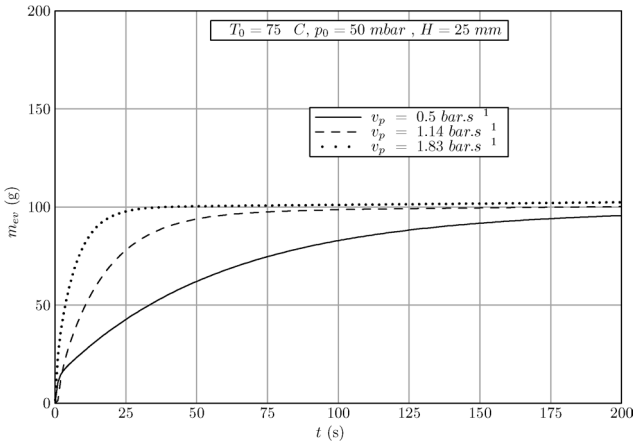

Fig. 14. Evolution of the evaporated mass with time for $T_0 = 75\,°C$, $p_0 = 50$ mbar and various initial temperatures and initial levels of liquid.

height of liquid initially placed in the flash chamber decreases.

4.3.2. Evolution of the flashing time with the depressurization rate

Fig. 13 presents the evolution of the flashing time with the depressurization rate for initial temperatures of 60 °C, an initial pressure of 50 mbar and initial heights of distilled water of 25, 100, 150, and 250 mm. This flashing time is estimated using the method initially introduced by Miyatake et al. [13, 14], based on the NEF evolution with time and briefly described previously in this article. For other temperatures and pressure the same trend is observed.

In a general way, for a given T_0, p_0 and H, this time is a decreasing function of the increasing rate of depressurization. For the same initial temperature and pressure this time augments with the increase of the initial water level. That confirms observations made in the previous paragraph: equilibrium state is reached slower when the initial water level increases. Indeed, in our case, an increase of the initial water level entails an increase of the initial volume of the water placed in the flash chamber. Thus, the water volume to cool is more significant and it is thus not surprising that characteristic time of the phenomenon would be more significant when increasing the water level.

4.3.3. Evolution of the total evaporated mass with time

Fig. 14 plots the evolution of the mass evaporated versus time for an initial temperature of 75 °C, an initial pressure in the vacuum tank p_0 of 50 mbar, and an initial water height of 25 mm. For other initial temperatures and heights, the same behavior as for $T_0 = 75\,°C$ could be observed, but these curves are not presented here.

In a general way, this total evaporated mass is an increasing function of time. Moreover, whatever the initial height of liquid, the higher the rate of depressurization, the faster the final evaporated mass m_{ev}^f ($m_{\mathrm{ev}}^f = \lim_{t\to\infty} m_{\mathrm{ev}}(t)$) is reached. Moreover, as observed for *NEF*, we also observe that when the initial water level decreases, profiles are more "square", which correspond to a faster phenomenon. Indeed, like previously, the volume of water to cool is lower which implies a faster phenomenon. This also explains the evolution of the profiles with the initial height of distilled water.

4.3.4. Evolution of the final mass evaporated by flashing with the depressurization rate

Fig. 15 shows the evolution of the final mass evaporated with the rate of depressurization for an initial pressure in the vacuum tank of 50 mbar, an initial temperature of 75 °C and

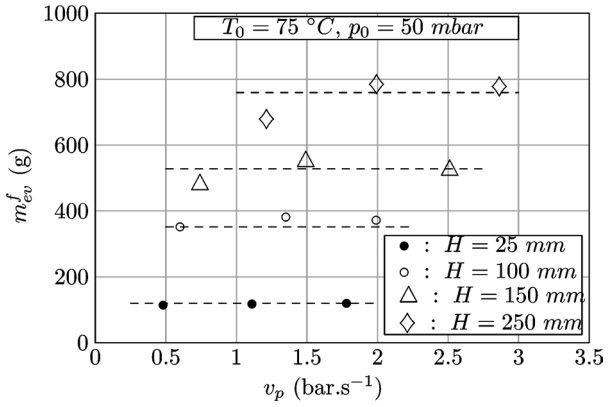

Fig. 15. Evolution of the final mass evaporated with the rate of depressurization for $T_0 = 75\,°C$, $p_0 = 50$ mbar and various initial temperatures and initial levels of liquid.

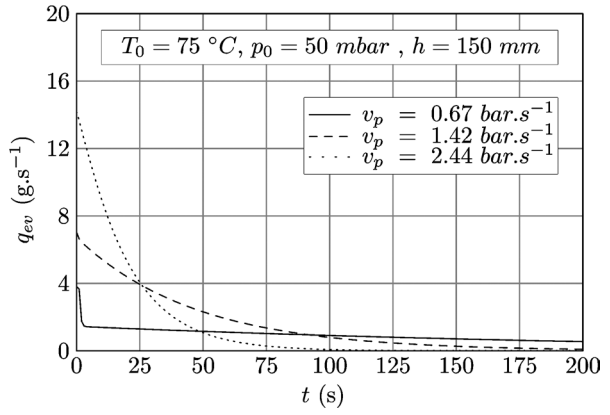

Fig. 16. Evolution of the evaporated mass flow rate with time.

various initial temperatures and heights of distilled water. The same behavior is observed for others experiments carried out. Results show that whatever the initial temperature, this mass is, for a given initial height of distilled water and initial pressure, independent of the depressurization rate.

4.3.5. Evolution of the evaporated mass flow rate with time

Fig. 16 presents the evolution of the mass flow rate with time for an initial temperature of 75 °C, an initial pressure p_0 of 50 mbar, and initial water height of 150 mm. We do not present here the curves corresponding to the other initial temperatures heights, for which the same trend can be observed.

As show on this graph, the evaporated mass flow rate is a decreasing function of time, this decrease being controlled by the depressurization rate. Indeed, whatever the initial height of liquid, the higher the initial rate of depressurization will be, the faster the value of the evaporated mass flow rate will decrease. We can moreover notice that the higher the initial rate of depressurization, the more significant the initial value of this flow rate. Indeed, the evaporated total mass m^f_{ev} is represented (apart from the scale factor) by the area below the curve representing the mass flow rate versus time ($m^f_{\mathrm{ev}} = \int_0^\infty q_{\mathrm{ev}}(t)\,\mathrm{d}t$). In addition, we noted previously

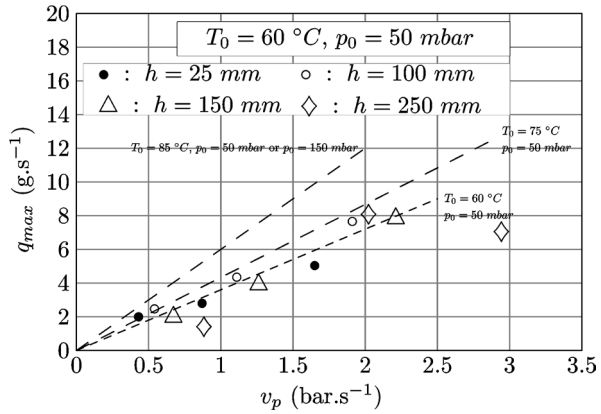

Fig. 17. Evolution of the initial evaporated mass flow rate with the depressurization rate for a pressure in the vacuum tank of 50 mbar, an initial temperature of 60 °C and various initial liquid levels.

that this mass whose value depends mainly on the superheat (cf. [17]) and on the water mass initially placed in the flash chamber is independent of the depressurization rate. Thus, for a given initial height, the surface under each curve must be equal and thus a fast decrease must be compensated by a higher initial value of the evaporated mass flow rate.

4.3.6. Evolution of the initial flow with the depressurization rate

Fig. 17 plots the evolution of the maximum mass flow rate evaporated versus the depressurization rate for initial temperatures of 60 °C, an initial pressure in the vacuum tank of 50 mbar and initial water heights of 25, 100, 150, and 250 mm. Analyze of the evolution of the evaporated mass flow rate with time shows this value corresponds to the initial value of the mass flow rate.

In a general way, we note an increasing of the maximum evaporated mass flow rate with the initial depressurization rate in the flash chamber. Moreover, for a given initial temperature and a given initial pressure, evolution of this mass flow rate with the initial rate of depressurization is relatively linear whatever the level of distilled water initially put in the flash chamber. In addition, On this graph, we also add slopes of the approximation straight line found for other temperatures (75 and 85 °C). As observed, these slopes increase with the initial temperature (T_0). This is due to the fact that increases T_0 promotes bubbles formation and growth (critical radius of bubble formation decreases with temperature, then the number of viable bubbles increases) and then vapor formation. It explains that, initially, mass flow rate would be greater. Globally, this mass flow rate significantly growths with the increase of the depressurization rate and with the one of the initial temperature. Results obtained shows that the mass flow rate is a linear function of v_p and depends also on T_0, i.e. $q_{\max} = \mathcal{F}(T_0)v_p$.

These results show that if we wish optimize the mass evaporated in industrial processes using the flashing, successive flashing let increase these evaporated masses significantly. These different flashing having to be spaced of t^*,

since we remark that it is in the first step ($t \leqslant t^*$) that the evaporated mass flow rate is most significant and that it becomes relatively low for $t \gg t^*$. We also could note that, the faster the depressurizations, the lower the flashing time and thus the more we can, in a given time, carry out a significant number of successive vacuum settings (within the possible material limits: time to warming up again the liquid and to re-lowering the pressure in the vacuum tank).

5. Synthesis

Dimensional analysis [25] introduces dimensionless numbers for each physical quantity. Correlations describing evolution of $q_{\max}$, t^*, or m^* versus other dimensionless significant parameters (T_0, v_p, ΔT, or H) were found. As this study is carried out on distilled water having an initial temperature ranging between 45 and 85 °C, a initial water level from 25 to 250 mm, an initial pressure in the vacuum tank of 50 and 150 mbar and depressurization rate ranging between 0 and 3.5 bar·s^{-1}, which globally correspond to a superheat 0 and 44 K. These values correspond to the range of validity of these following correlations.

A correlation between the dimensionless maximum mass flow rate $\overline{q_{\max}}$ and dimensionless initial temperature $\overline{T_0}$, depressurization rate $\overline{v}_p$, superheat $\overline{\Delta T}$, initial water height $\overline{H}$ is proposed.

$$\overline{q_{\max}} = \mathcal{K} \times \overline{T_0}^{2.62} \times \overline{v_p}^{1.14} \times \overline{\Delta T}^{-0.05} \times \overline{H}^{0.01} \tag{10}$$

where

$$\mathcal{K} = 9.689 \times 10^{-4}$$

$$\overline{q_{\max}} = \frac{q_{\max}}{\mu(T_0) D}$$

$$\overline{T_0} = \frac{c_p(T_0)(T_0 - T_{\text{ref}})}{g D}$$

$$\overline{v_p} = \frac{v_p D}{\mu(T_0) g}$$

$$\overline{\Delta T} = \frac{c_p \Delta T}{h_{\text{fg}}(T_0)} = Ja$$

$$\overline{H} = \frac{H}{D}$$

and where $T_{\text{ref}} = 273$ K, and v_p is in bar·s^{-1} other quantities being in SI units.

Range of validity of this latter correlation is specified below: $T_0 \in [45, 85\,^\circ\text{C}]$, $v_p \in [0, 3.5\ \text{bar·s}^{-1}]$, $\Delta T \in [0, 45\ \text{K}]$, $H \in [0, 250\ \text{mm}]$. Fig. 18 plots evolution of the maximal mass flow rate evaporated versus parameters presented before. As shown on this figure, the correlation proposed described relatively well evolution of this mass flow rate. Correlation coefficient obtained is 0.92. We also find again what observed before, i.e., $q_{\max} \approx \mathcal{F}(T_0) \times v_p$ since power above the dimensionless quantities relative to the initial water height and the superheat are almost zero which entails a very weak influence of those terms. Moreover, power relative to v_p is almost 1 which confirms quasi-linear trend observed before on Fig. 17. We also point out again influence of the initial temperature still observed on Fig. 17. In addition, this correlation lets quantify influence effect of studied parameters. As shown, influence of the superheat and of the initial water height is very restricted, that's why comparison between this latter correlation (Eq. (10) and a more simple law ($\overline{q'_{\max}} = \mathcal{F}(\overline{T_0}, \overline{v_p})$) is realized. Correlation obtained is proposed below:

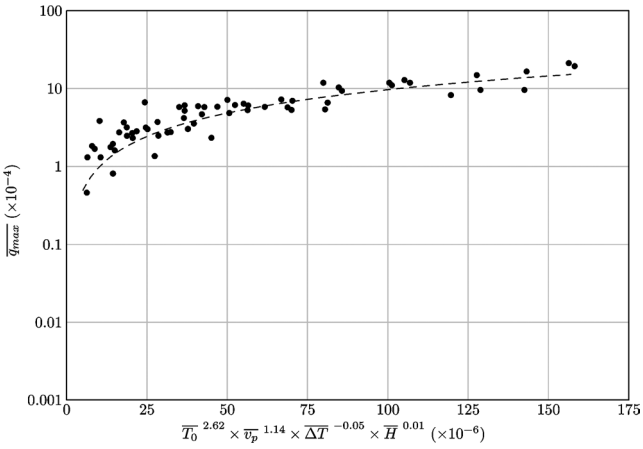

Fig. 18. Evolution of the maximal mass flow rate.

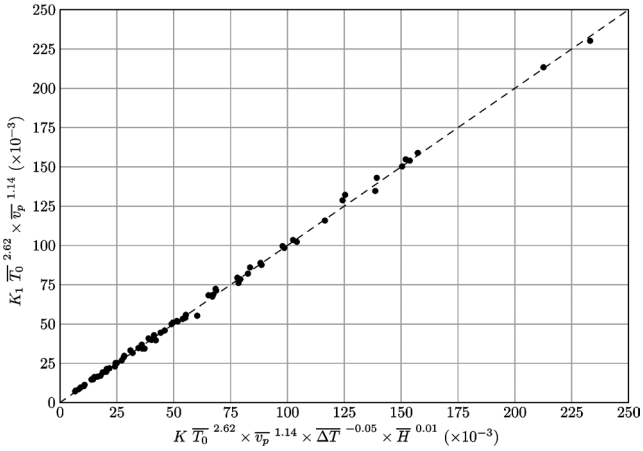

Fig. 19. Comparison between $q_{\max}$ and $q'_{\max}$.

$$\overline{q'_{\max}} = \mathcal{K}_1 \times \overline{T_0}^{2.62} \times \overline{v_p}^{1.14} \quad \text{with } \mathcal{K}_1 = 1.124 \times 10^{-3} \tag{11}$$

Relative error made by using Eq. (11) instead of Eq. (10) remains lower than 10%. Fig. 19 plots Eq. (10) versus Eq. (11). This graph shows a good agreement between this two correlations in their range of validity.

From the study of flashing time with various initial conditions, we determined a correlation between the dimensionless flashing time ($\overline{t^*}$) and the main dimensionless parameters described before ($\overline{T_0}$, $\overline{v_p}$, $\overline{\Delta T}$, $\overline{H}$).

$$\overline{t^*} = \mathcal{K}' \times \overline{T_0}^{3.16} \times \overline{v_p}^{-0.83} \times \overline{\Delta T}^{2.45} \times \overline{H}^{1.07} \tag{12}$$

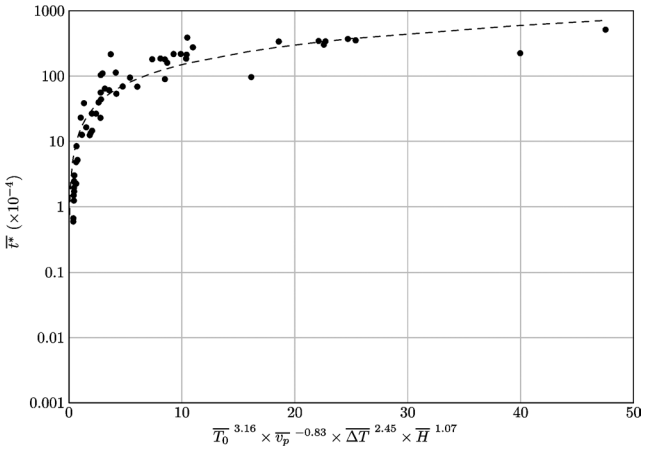

Fig. 20. Evolution of the flashing time.

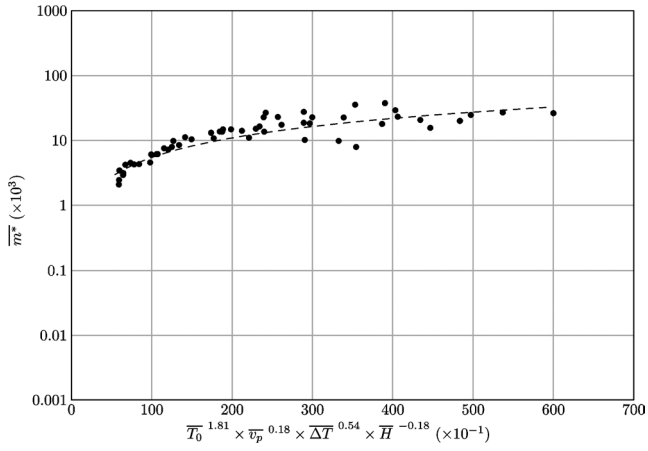

Fig. 21. Evolution of the mass evaporated at time t^*.

where: $\mathcal{K}' = 1.496$, $\overline{t^*} = t^*/\tau$, $\tau = \frac{\rho c_p \sigma^2}{\lambda(\Delta p)^2}$ and $\overline{T_0}$, $\overline{v_p}$, $\overline{\Delta T}$, $\overline{H}$ are the same as previously.

The range of validity of this correlation is the same as for the previous correlation, i.e., $T_0 \in [45, 85\,^\circ\text{C}]$, $v_p \in [0, 3.5\ \text{bar}\cdot\text{s}^{-1}]$, $\Delta T \in [0, 45\ \text{K}]$, $H \in [0, 250\ \text{mm}]$.

Fig. 20 plots results obtained experimentally and those obtained with the correlation Eq. (12). A pretty good agreement can be noticed. Moreover, correlation coefficient between experimental results and correlation is 0.97. As previously, this correlation confirms trends observed and explained before, as known: t^* decreases with v_p and increases with H. This time increases with the superheat which probably could be explained by the fact that increasing ΔT is as increasing energy amount to convert into latent heat of vaporization, other parameters being not changed. In addition, this trend confirms also what Miyatake observed in its correlation about the flashing time [13,14], even if correlation he proposed does not take into account the rate of depressurization ($t^* = 44 T_e^{-0.86} \Delta T^{0.55}$, [13]).

From analysis of results about the water mass evaporated with various initial conditions, we determined a correlation between the dimensionless mass evaporated at time t^* ($\overline{m^*}$) and the main dimensionless parameters described before ($\overline{T_0}$, $\overline{v_p}$, $\overline{\Delta T}$, $\overline{H}$).

$$\overline{m^*} = \mathcal{K}'' \times \overline{T_0}^{1.81} \times \overline{v_p}^{0.18} \times \overline{\Delta T}^{0.54} \times \overline{H}^{-0.18} \tag{13}$$

where: $\mathcal{K}'' = 5.466 \times 10^{-6}$, $\overline{m^*} = m^*/m_0$, $\overline{T_0}$, $\overline{v_p}$, $\overline{\Delta T}$, $\overline{H}$ being the same as previously. The range of validity for this correlation is $T_0 \in [45, 85\,^\circ\text{C}]$, $v_p \in [0, 3.5\ \text{bar}\cdot\text{s}^{-1}]$, $\Delta T \in [0, 45\ \text{K}]$, $H \in [0, 250\ \text{mm}]$.

Fig. 21 plots results we obtain both experimentally and using the correlation Eq. (13) versus main dimensionless parameters ($\overline{T_0}$, $\overline{v_p}$, $\overline{\Delta T}$, $\overline{H}$). Value of the correlation coefficient between experimental results and this latter correlation is 0.92 and shows a good agreement between these values. As for others correlations, this correlation allows to see influence of parameters such as T_0, v_p, ΔT or H on the mass evaporated at time t^*. For instance, m^* increases with T_0 and slightly decreases with H even if influence of this latter parameter is not very significant (power -0.18 in Eq. (13)). For example, we can noticed that m^* increases with T_0 or v_p. Increasing T_0 or v_p increases the initial mass flow rate (see, for instance, Eq. (10)). So, slope of the curve plotting mass evaporated versus time growths faster and this mass tends more quickly towards its asymptotic value which corresponds to the final mass evaporated (m_{ev}^f). Then the mass evaporated at time t^* is greater which explains why m^* increases with T_0 and v_p.

Keeping in mind the range of validity of these tree correlations, we provide here first hints to optimized processes based on this phenomenon such as drying phase in case of sterilization of surgical instruments processes. Indeed, values of evaporated quantities and time to evaporate this quantities can be easily obtain using these correlations and a compromise between each parameter can be found.

6. Conclusion

This article presents both an experimental study of the influence of the initial water level in the flash chamber and of the depressurization rate on the flash evaporation phenomenon. This study is carried out on distilled water having an initial temperature ranging between 45 and 85 °C, a initial water level from 25 to 250 mm, and an initial pressure in the vacuum tank of 50 and 150 mbar. Initially, we present a qualitative approach of flash evaporation, consisting in a visualization of the flashing phenomenon using a CCD camera. This visualization lets us highlight the influence of initial height of liquid on its flash evaporation. A quantitative approach is then proposed. This approach is based on the use of the energy balance on the liquid in the flash chamber and on temperature measurement of the water. This study allows us to show that the maximum amplitude of the flash evaporation phenomenon, the flashing time, as well as the final evaporated mass are increasing functions of the initial liquid level. In addition, by introducing the ratio of the evaporated masses at the moment t^*, and at end, we highlight the

importance of the pressure drop on the effectiveness of the phenomenon.

We also propose an experimental study of the influence of the depressurization rate on the flash evaporation of a water film. This study is carried out with initial temperature of water film of 60, 75, and 85 °C. Runs with initial heights of distilled water of 25, 100, 150 and 250 mm and a pressure in the vacuum tank of 50 and 150 mbar were carried out. The study of the main physical quantities enables us to point out the influence of the depressurization rates on the temporal NEF evolution, on the mass and the mass flow rate evaporated. Study of NEF lets us determine the flashing time t^*, thus we found a lower flashing time when the rate of depressurization is increased. Moreover, the evolution of the mass evaporated with time allows us to determine the final mass evaporated by flashing. Then we remark that this mass is almost independent of the depressurization rate. Finally, the study of the maximum value of the evaporated mass flow rate allows us to highlight a relatively linear evolution of this flow rate with the depressurization rate for a given initial temperature and initial pressure.

Runs carried out with various initial conditions let us correlate, in a more general way, the maximal value of the dimensionless mass flow rate, the dimensionless flashing time or the dimensionless water mass evaporated at time t^* with the dimensionless parameters influencing the phenomenon, i.e., the initial temperature, the superheat, the depressurization rate, the initial level of liquid, and the liquid surface undergoing the pressure drop. These correlations, from which we can predict influence of such or such parameter, can be used to optimize industrial processes based on flash evaporation phenomenon.

In future, we plan to confirm results obtained with different fluids (salted water, ...). In addition, it would be interesting to analyse fundamental aspects of the bubble formation in order to predict in another way the mass flow rate.

References

[1] K. Spiegler, Y. El-Sayed, The energetics of desalination processes, Desalination 134 (2001) 109–128.

[2] O. Miyatake, Y. Koito, K. Tagawa, Y. Maruta, Transient characteristics and performance of a novel desalination system based on heat storage and spray flashing, Desalination 137 (2001) 157–166.

[3] M. Balistrou, S. Harmand, B. Desmet, Étude des phénomènes de transferts thermiques dans les stérilisateurs à vapeur, Rev. Gén. Thermique 35 (418–419) (1996) 686–692.

[4] A. Woods, F. Bloom, Modelling of flash evaporation i: Formulation of the mathematical model, Math. Comput. Modelling 32 (2000) 1153–1169.

[5] I. Aoki, Water flash evaporation under low pressure conditions, Heat Transfer Japan. Res. 23 (6) (1994) 544–555.

[6] I. Aoki, Analysis of characteristics of water flash evaporation under low-pressure conditions, Heat Transfer Asian Res. 29 (1) (2000) 22–33.

[7] P. Sebastian, J. Nadeau, Experiments and modelling of falling jet flash evaporators for vintage treatment, Internat. J. Thermal Sci. 41 (2002) 269–280.

[8] U. Desderi, G. Bidini, Study of possible optimisation criteria for geothermal power plants, Energy Convers. Mgmt. 38 (15–17) (1997) 1681–1691.

[9] H. Shokoumand, P. Atashkadi, Performance improvement of single, flashing, binary, combined cycle for geothermal powerplant, Energy 22 (7) (1997) 637–643.

[10] U. Colak, O. Özdere, Comparative analysis of pressure vessel integrity for various loca conditions, J. Nuclear Material 297 (2001) 271–278.

[11] H.K. Pulker, Flash evaporation, Vakuum Forschung Praxis 3 (2000) 197–198.

[12] R. Peterson, S. Grewal, M. El-Wakil, Investigations of liquid flashing and evaporation due to sudden depressurization, Internat. J. Heat Mass Transfer 27 (2) (1984) 301–310.

[13] O. Miyatake, K. Murakami, Y. Kawata, T. Fujii, Fundamental experiments with flash evaporation, Heat Transfer Japan. Res. 2 (1973) 89–100.

[14] O. Miyatake, T. Fujii, T. Tanaka, T. Nakaoka, Flash evaporation phenomena of pool water, Heat Transfer Japan. Res. 6 (1977) 13–24.

[15] S. Gopalakrishna, V.M. Purushothaman, N. Lior, An experimental study of flash evaporation from liquid pools, Desalination 65 (1987) 139–151.

[16] S. Gopalakrishna, Studies on enclosed pool flash evaporation, PhD thesis, University of Pennsylvania, 1989.

[17] D. Saury, S. Harmand, M. Siroux, Experimental study of flash evaporation of a water film, Internat. J. Heat Mass Transfer 45 (16) (2002) 3447–3457.

[18] E. Hahne, G. Barthau, Evaporation waves in flashing processes, Internat. J. Multiphase Flow 26 (2000) 531–547.

[19] J. Bartak, A study of the rapid depressurization of hot water and the dynamics of vapour bubble generation in superheated water, Internat. J. Multiphase Flow 16 (5) (1990) 789–798.

[20] E. Elias, P.L. Chambré, Flashing inception in water during rapid decompression, ASME J. Heat Transfer 115 (1993) 231–238.

[21] M. Alamgir, C.Y. Kan, J. Lienhard, An experimental study of the rapid depressurization of hot water, ASME J. Heat Transfer 102 (1980) 433–438.

[22] M. Alamgir, J. Lienhard, Correlation of pressure undershoot during hot water depressurization, ASME J. Heat Transfer 103 (1981) 52–55.

[23] P. Reinke, G. Yadigaroglu, Explosive vaporization of superheated liquids by boiling fronts, Internat. J. Multiphase Flow 27 (2001) 1487–1516.

[24] P. Deligiannis, J.W. Cleaver, The role of nucleation in the initial phases of rapid depressurization of a subcooled liquid, Internat. J. Multiphase Flow 16 (6) (1990) 975–984.

[25] D. Saury, Etude expérimentale de l'évaporation flash d'un film d'eau, Thèse en énergétique, n d'ordre 03/19, Université de Valenciennes et du Hainaut-Cambrésis, 2003.

[26] J. Kim, N. Lior, Some critical transitions in pool flash evaporation, Internat. J. Heat Mass Transfer 40 (10) (1997) 2363–2372.